

# FEEDBACK SYSTEM DESIGN TECHNIQUES FOR CONTROL OF INTRA-BUNCH INSTABILITIES AT THE SPS\*

C. H. Rivetta<sup>†</sup>, J. Cesaratto, J. Dusatko, J. D. Fox, O. Turgut, SLAC, Stanford CA, USA  
 W. Hofle, K. Li, G. Kotzian, CERN, Geneva, Switzerland

## Abstract

The feedback control of intra-bunch instabilities driven by electron-clouds or strong head-tail coupling requires bandwidth sufficient to sense the vertical position and apply multiple corrections within a nanosecond-scale bunch. These requirements impose challenges and limits in the design and implementation of the feedback system. This paper presents model-based design techniques for feedback systems to address the stabilization of the transverse bunch dynamics. These techniques include in the design the effect of noise and signals perturbing the bunch motion. Different controllers are compared based on stability margins and equivalent noise gain between input-output of the processing channel. The controller design uses as example the bunch dynamics defined by the SPS ring including the Q20 optics.

## INTRODUCTION

The feedback control of intra-bunch instabilities induced by electron-cloud (ECI) or strong head-tail interaction (transverse mode coupled instabilities TMCI) requires enough bandwidth to sense the vertical position motion and apply correction fields to multiple sections of a nanosecond-scale bunch. This paper addresses the design of the controller to stabilize the intra-bunch dynamics of the beam at SPS assuming it includes the Q20 optics. This requirement impose challenges because the optics define a synchrotron frequency  $\omega_s = 0.0170$ , spreading out the frequency of the satellite bands around the betatron frequency  $\omega_\beta = 0.185$ . Feedback control model-based design techniques allows to assess the system stability and address the system performance including in the controller design the rejection to noise and perturbations. The control feedback assumed for this application is based on a digital reprogrammable architecture, sampling the bunch motion at a rate of 4 GS/s. Different controller filters are proposed and compared based on the system stability criteria and the equivalent noise gain between the input-output of the filter.

## ANALYSIS OF INTRA-BUNCH INSTABILITIES

Studies of instabilities induced by electron-cloud and strong head-tail coupling have been carried out using macro-particle simulation codes [1]. Detailed analysis using two different optics, Q20 and Q26 were conducted and some results for the Q20 lattice are shown in Figs 1 and 2. The

first figure shows the result of increasing electron cloud density on the bunch motion or instability. This plot shows the magnitude of the vertical motion for different modes for a bunch charge equal to  $1.1 \times 10^{11}$  ppb,  $E = 26$  GeV/c and chromaticity equal to zero. Fig. 2 shows effect of the interaction of the bunch with the machine impedance for increasing bunch charge,  $E = 26$  GeV/c and chromaticity equal to zero. From these plots it is possible to observe the in the case of electron cloud driven instabilities the first upper satellite band becomes unstable when the electron cloud density is  $\approx 12.3 \times 10^{11} \text{ m}^{-3}$  and the frequency of each mode increases with the electron cloud density. For TMCI, mode -2 becomes unstable at a bunch intensity  $\approx 4 \times 10^{11}$  ppb and the frequency of the modes decreases for increasing bunch intensity. This information is particularly useful in the design of feedback controllers to assess the bunch stability and the robustness of the damper system to changes in the operation conditions.

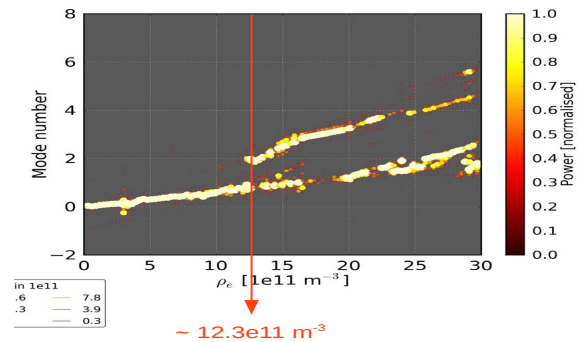


Figure 1: Bunch vertical motion for increasing electron cloud densities.

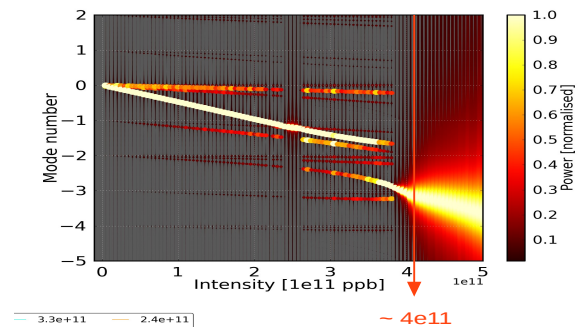


Figure 2: Bunch vertical motion for increasing bunch intensity.

\* Work supported by the U.S. Department of Energy under contract DE-AC02-76SF00515 and the US LHC Accelerator Research Program LARP  
<sup>†</sup> rivetta@slac.stanford.edu

## DESIGN CRITERIA OF THE CONTROL FEEDBACK

The first requirement for the controller is to stabilize the intra-bunch dynamics driven by electron cloud and strong head-tail instabilities. Additionally, the feedback system has to be robust to parameter changes in the beam dynamics and different operation conditions of the machine. The controller has to have enough dynamic range to keep the stability-performance of the system for a maximum set of beam transient conditions. Given the conditions that the open loop system is unstable and the feedback channel has delay, these could exist a combination of fast unstable dynamics and long delay in the system that makes the controller unfeasible. The bandwidth of the controller has to be limited to minimize the effect of the receiver noise in the saturation of the power stage. Additionally, the filter has to be able to reject signal perturbations that affects the performance of the feedback system.

A topology used to implement the feedback system consists of a digital processing channel based on a reconfigurable FPGA and ADC/DACs operating at 3.2 GS/s [2]. A general block diagram of the proposed hardware is depicted in Fig. 3. Analog equalization of the pick-up and cable transfer function is included in the feedback channel. The controller is implemented using a bank of FIR / IIR filters, processing each individual ADC samples across the bunch. Based on a reduced model of the bunch dynamics it is possible to design a stabilizing controller based on the criteria defined in the paragraph above.

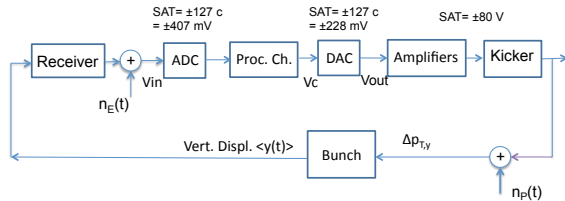


Figure 3: Block diagram control feedback system.

The bunch dynamics is characterized by dominant modes whose eigenvalues are  $\pm i(\omega_\beta + k\omega_s)$  for  $k = \dots, -6, \dots, 0, \dots, +6, \dots$ . Conducting the analysis of the system in discrete time, with eigenvalues mapped in  $\mathcal{Z}$  domain to  $\sigma_k = e^{\pm i(\omega_\beta + k\omega_s)}$ . Taking the first six modes as the dominant ones in the bunch dynamics, Fig. 4 shows the location of those eigenvalues in the complex plane. The controller filter have to include different sections to fulfill the design criteria presented above. It includes a zero at  $z = 1 + i 0$  to reject the revolution harmonics in the signal due to the vertical offset of the beam. A low-pass Chebyshev filter is included to attenuate high frequency signals and noise. Multiple zeros are included in the filter to produce the necessary damping around the dominant dynamics of the bunch that if necessary to damp. The location of poles-zeros of a generic controller filter is depicted also in Fig. 4.

We evaluate the filter design considering  $\pm 6$  lateral bands around the betatron frequency. Setting the filter architecture,

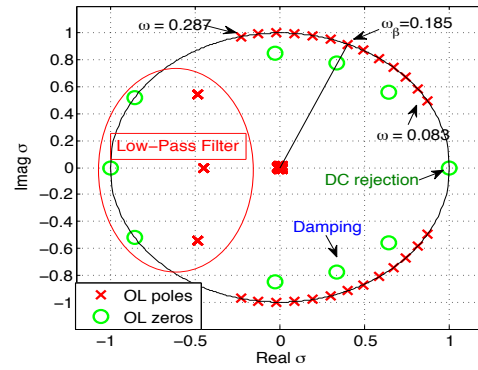


Figure 4: Pole-zero location for filter and dominant bunch dynamics.

different filters are analyzed by changing the numbers of zeros and the bandwidth of a common third order low-pass Chebyshev-II filter. The critical parameters in the design are the low-pass bandwidth, the position of zeros and the adjustment of the overall phase. These parameters are adjusted based on the stability margin of the feedback system and the equivalent noise gain between input and output of the controller. The transfer function of the filters used in this analysis are depicted in Fig. 5 for controllers including 1 to 3 zeros to introduce damping and they are compared with the case where no zeros are included. It is important to observe that the phase of the filter is about  $-270^\circ$  in a frequency span around the fractional betatron tune  $\omega_\beta = 0.185$  producing damping in the system.

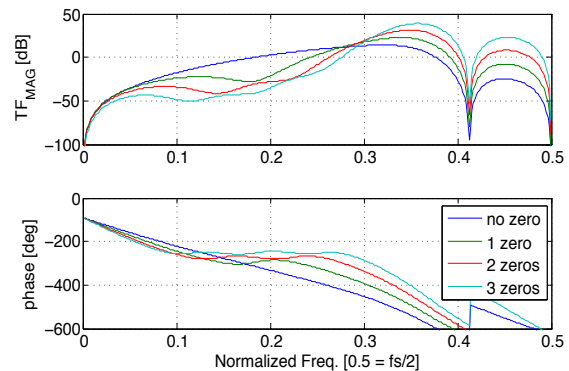


Figure 5: Controller filter transfer functions.

### Stability Analysis

To evaluate the stability we use the root locus technique, where the eigenvalues of the closed loop system are plotted for different gain in the controller ( $G = 0, \dots, G_{max}$ ). In the case on discrete systems, the eigenvalues  $\sigma$  inside the unitary circle defines a stable system. Fig. 6 depicts the root locus when the controller has a filter with a single zero. Blue dots represent the closed loop eigenvalues for different gains. Red crosses define the poles in open loop ( $G = 0$ ), while the cyan crosses define the closed loop eigenvalues at the selected gain  $G_f$ . It is assumed that the chromaticity is equal to zero.

A detail of the root locus around the upper part of the plot is depicted in Fig. 7. Similarly, Fig. 8 show the detail of the root locus for a controller implemented with a filter including 3 zeros. Similar results were evaluated for filters with 2 zeros. In those designs the position of the zeros and the bandwidth of the low-pass filter was adjusted and the selected gain  $G_f$  is defined to set the same damping for mode 0 (Damping  $\approx 20$  turns, black dashed lines) and similar stability margins. To compare the different implementations, we evaluated the impact on those filters in the noise amplification between the input to output of the controller.

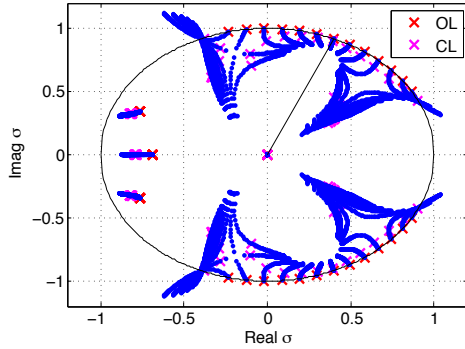


Figure 6: Complete root-locus for the feedback system including a controller with one zero filter.

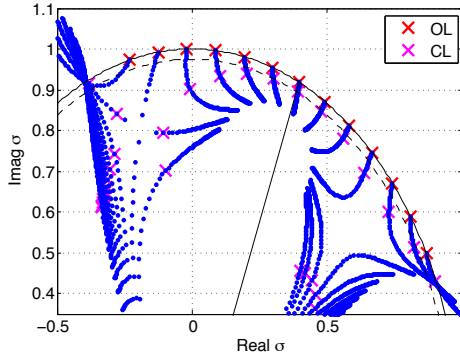


Figure 7: Detail of root-locus for the feedback system including a controller with two zero filter.

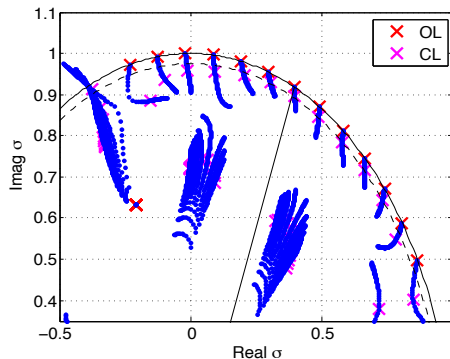


Figure 8: Detail of root-locus for the feedback system including a controller with three zero filter.

## Equivalent Noise Gain

Let us define the ratio between input to output of the filter in frequency domain by  $V_{out}(i\omega) = G_{fil}(i\omega)V_{in}(i\omega)$ . If we consider that the input signal is white noise with power equal to  $\sigma_{in}^2$ , then for the output signal

$$\begin{aligned}\sigma_{out}^2 &= G_2^2 \sigma_{in}^2 \\ &= \frac{1}{2\pi} \int_{-\infty}^{\infty} V_{in}^*(i\omega) G_{fil}^T(-i\omega) G_{fil}(i\omega) V_{in}(i\omega) d\omega \\ &\leq \left( \sup_{\omega \in \mathcal{R}} \|G_{fil}(i\omega)\|_2 \right)^2 \sigma_{in}^2\end{aligned}$$

The results for the different filters are

- IIR 1 zero:  $BW_{LP}=0.9$ ,  $G_f=575$ ,  $G_2=770$
- IIR 2 zeros:  $BW_{LP}=0.8$ ,  $G_f=639$ ,  $G_2=588$
- IIR 3 zeros:  $BW_{LP}=0.7$ ,  $G_f=1086$ ,  $G_2=543$

This preliminary analysis show that filter with larger numbers of zeros allow assessing the stability limits with minimum equivalent noise gain between input-output of the controller. Additional constrains in the design must be included as the effect of hardware limits and bandwidth, etc. to evaluate a more realistic design of the control feedback. One of the main constraints is the balance in the system design among the received and quantizing noise, the equivalent noise gain of the filter and the maximum power of the driver amplifier. This issue is the next in the design toward the final filter architecture to be included in the controller FPGA.

## CONCLUSIONS

We started evaluating a design for the feedback controller for the SPS ring including the Q20 optics. It imposes a challenge due to the large synchrotron frequency  $\omega_s$ , spreading out in a wide frequency band the dominant modes of the bunch. Multiple filters have been analyzed using the criteria the system stability and the noise gain of the filter. Future work will include improvement in the reduced model of the beam to optimize the controller design, add in the feedback system more realistic models of the hardware, analyze limitations and partition the gain around the feedback loop. In parallel, these work will be evaluated using macro-particle simulation codes to validate models and study different operation conditions of the machine.

## REFERENCES

- [1] K. Li, et al., "Modeling and Studies for a Wideband Feedback System for Mitigation of Transverse Single Bunch Instabilities", WEPME042, IPAC13, Shanghai, China, (2013).
- [2] J. D. Fox, et al., "The Hardware Implementation of the CERN SPS Ultrafast Feedback Processor Demonstrator", MOPC28, IBIC13, Oxford, UK, (2013).